PEGylated Interferon Displays Differences in Plasma Clearance and Bioavailability Between Male and Female Mice and Between Female Immunocompetent C57Bl/6J and Athymic Nude Mice

CORNELIA B. LANDERSDORFER,[1] SUZANNE M. CALIPH,[1] DAVID M. SHACKLEFORD,[1] DAVID B. ASCHER,[2] LISA M. KAMINSKAS[1]

[1]Drug Delivery Disposition and Dynamics, Monash Institute of Pharmaceutical Sciences, Parkville, Victoria 3052, Australia
[2]Department of Biochemistry, University of Cambridge, Cambridge CB21GA, United Kingdom

ABSTRACT: Gender and immune status can considerably impact on the pharmacokinetics (PK) of macromolecular and small molecule drugs. However, these effects are often not considered in drug development. We aimed to quantitatively evaluate effects of gender and immune status on the PK of PEGylated interferon in frequently used murine models. Chronically cannulated female athymic nude and female and male immunocompetent C57Bl/6J mice ($n = 24$ in total) received a single intravenous or subcutaneous (s.c.) dose of PEGylated interferon. Serial blood samples were taken for 48 h. Noncompartmental analysis and population PK modeling with covariate analysis were performed to evaluate the data. The PK of PEGylated interferon followed a three compartment disposition model with two sequential compartments for s.c. absorption. Female nude mice had significantly higher plasma clearance than C57Bl/6J mice (0.503 vs. 0.397 mL/h). Male mice had a slower absorption rate constant (0.138 h^{-1}) and extent (46.2%) of s.c. absorption than female mice (0.274 in C57Bl/6J and 0.374 h^{-1} in nude, 60.8% in both). Thus, gender and immune status significantly impacted on important PK parameters of PEGylated interferon in murine models commonly utilized in drug development. It is critical to take into account these differences when choosing animal models and conducting translational pharmacology research. © 2015 Wiley Periodicals, Inc. and the American Pharmacists Association J Pharm Sci 104:1848–1855, 2015
Keywords: pharmacokinetics; macromolecular drug delivery; pegylation; gender; population pharmacokinetics; mathematical model; bioavailability; absorption; elimination

INTRODUCTION

In spite of the potential impact of gender on drug disposition (and in turn, efficacy),[1] the issue is often overlooked in drug development to the extent that in many instances the standard protocol has been to use only male animals for preclinical studies. This is often justified on the basis of "reducing the variability associated with fluctuations in hormone levels."[1,2] In a push to overcome the potential failings associated with male-biased preclinical studies, the European Commission, the Canadian Institutes of Health, and the US National Institutes of Health have recently implemented policy changes to ensure that both male and female cells and animals are used in preclinical drug development initiatives funded by these agencies.[2] There remains, however, a paucity of information and only a limited number of examples of gender differences in drug pharmacokinetics (PK) in preclinical species. It is reasonable to expect that such differences exist; however, given that at the most fundamental level, we have previously shown that the underlying physiology involved in drug uptake in rodents can vary between the genders, and even between strains.[3]

Although the rate of small molecule therapies reaching the market has slowed, there has been an increasing number of macromolecular drugs and drug delivery systems entering the market and late phase clinical trials, particularly for the treatment of cancer. Macromolecular drugs include protein thera-

peutics (such as cytokines and antibodies), protein–drug conjugates (e.g., Kadcyla), nanoparticles (Abraxane), and colloids (Doxil, Myocet, Daunoxome). These macromolecules present unique PK challenges that could potentially make them very susceptible to gender differences. Specifically, they are generally administered via (intravenous) i.v. or subcutaneous (s.c.) delivery and are therefore potentially subject to an even greater plethora of gender-related PK differences when compared with small molecules that are delivered orally. For instance, drug absorption from a s.c. injection site can be influenced by local fat, interstitial pressure, blood flow, and lymphatic flow, which can all vary between males and females.[1,4–6] In addition, long-circulating macromolecules display significant lymphatic exposure and are more avidly targeted toward macrophages of the mononuclear phagocyte system (MPS). This is significant as macrophage function and subtype populations differ between males and females, and can have an important impact on the PK of macromolecules.[7] Given the generally very high cost of macromolecular drugs, it is important to understand early on in the development process the impact of gender on PK and pharmacodynamic (PD) outcomes in preclinical rodent models.[8]

Another complication that arises in the characterization of new molecules is that often different animal strains and even species are used to measure PK and PD properties. This is an important consideration, particularly in the development of chemotherapeutic macromolecules, where potential PK differences between rodent species and strains can complicate PK/PD simulations, when PK and PD are evaluated in different animal models. For instance, the PK of new macromolecular chemotherapeutics is generally characterized in fully

immunocompetent animals, whereas tumor efficacy studies are performed in immunocompromised nude mice that are deficient in T lymphocytes. Of particular importance to the PK and PD behavior of long-circulating macromolecules, the deficiency in T lymphocytes in nude mice appears to have an impact on the activity of macrophages that have to compensate for the loss of this important aspect of immunity.[9] Consequently, several studies have reported PK differences between nude and immunocompetent rodents.[10,11]

To this end, differences in immune cell function and populations between genders, and nude and immunocompetent animal models can have a profound impact on the PK of therapeutic cytokines (e.g., interferons) that have the potential to enhance immunosurveillance and chemotherapy for a variety of cancers. For instance, PEG–Intron® [interferon α2b conjugated with a single 12 kDa linear methoxy–polyethylene glycol (PEG) chain] displays intriguing gender-related effects on plasma PK and PD in different subject populations.[12–14] It is not known to this point, however, whether these PK differences in populations of humans with different immune function and gender can be predicted in basic rodent PK or PD models, and this formed the basis of the current study.

The aim of this study was to explore the hypothesis that the i.v. and s.c. PK of PEG–Intron® differs between male and female mice and between immunocompetent and nude mice. In particular, we hypothesized that after dosing via the s.c. route, PEG–Intron® would be subject to gender-related differences in absorption. This hypothesis was driven by the fact that a number of factors that are determinants of absorption from a s.c. injection site can vary between males and females[1,4–6] and also as differences in macrophage function and subtype populations differ between males and females and between nude and immunocompetent animals.[7] In addition, PEG–Intron® was examined here as it displays variable gender-related differences in s.c. PK in humans, is completely absorbed after s.c. administration in rats, and PEGylation has the potential to improve the exposure of lymphatic cancers to interferon and maximize chemotherapeutic activity.[15] To test this hypothesis, we used chronically cannulated female and male C57Bl/6J mice and female nude mice to enable the more robust collection of full PK data from individual animals. C57Bl/6J mice were used as immunocompetent controls as this is one of the most common mouse strains used in research and because this strain is generally favored in lymphatic PK research in mice. We used noncompartmental analysis and population modeling including covariate analysis to quantitatively evaluate differences in drug disposition and absorption.

MATERIALS AND METHODS

Materials and Reagents

PEG–Intron® (interferon α2b conjugated with a single linear 12 kDa PEG chain) was purchased from Schering-Plough (North Ryde, New South Wales, Australia) as the 150 µg/0.5 mL injectable REDIPEN®. The prepared solution was dispensed into sterile Eppendorf tubes as needed and stored at 4°C. Dosing solutions were prepared from this stock solution in sterile saline immediately before dosing. Sterile saline was from Baxter Pty Ltd. (Melbourne, Victoria, Australia). Polyvinyl tubing (inner diameter 0.2 mm, outer diameter 0.5 mm) was from Microtube Extrusions (New South Wales, Australia). An ELISA kit for the quantification of interferon 2α (PEGylated and native) was purchased from MabTech Australia Pty Ltd. (Macleod, Victoria, Australia). Carprieve (carprofen 50 mg/mL) was purchased from Norbrook Laboratories Australia (Tullamarine, Victoria, Australia) and Marcain (0.5% bupivacaine) was obtained from AstraZeneca (North Ryde, New South Wales, Australia). All other reagents were purchased from Sigma Chemical Company (New South Wales, Australia).

Animals

C57Bl/6J mice (10 weeks, $n = 8$ females weighing 21.4 ± 1.3 g, $n = 8$ males weighing 28.7 ± 2.0 g) were supplied by Monash Animal Services (Monash University, Victoria, Australia). Female athymic nude mice (10 weeks, $n = 8$, weight 19.8 ± 1.0 g) were supplied by the Animal Resources Centre (Western Australia, Australia). Animals were maintained on a 12-h light/dark cycle and were provided food and water at all times. Mice were acclimatized in mouse microisolator cages for 1 week prior to experimentation. All animal experimentation was approved by the Institutional Animal Ethics committee at the Monash Institute of Pharmaceutical Sciences.

Intravenous and Subcutaneous PK of PEG–Intron® in Mice

The plasma PK of PEG–Intron® was determined in carotid artery cannulated mice in order to obtain complete PK data within single animals. The cannulation procedure was essentially the same as the procedure reported previously for rats, with some modification. Briefly, mice were anaesthetized under isoflurane (2%) and the area around the incision sites and harness shaved (for C57 mice). The incision sites were cleaned with chlorhexidine and 50% ethanol, followed by 1% iodine (betadine). A total of 50 µL marcain was injected s.c. per mouse into the incision sites and carprofen (8 mg/kg) was given prior to surgery via s.c. administration into the left flank to provide postsurgical analgesia. The right carotid artery was then cannulated by inserting a 30-cm length of polyvinyl cannula that was prefilled with heparinized saline (3 IU/mL) 0.8 cm into the artery. The cannula was then exteriorized to the back of the neck and the wounds closed with 5/0 suture silk. Mice were then fitted with small jackets comprising soft latex that were affixed to metal swivel/tether harnesses (2 mm wide) via a small piece of Velcro. This enabled blood to be sampled from freely moving mice and at the same time, prevented mice from gaining access to the cannulas. Mice were then transferred into purpose built Perspex mouse metabolism units measuring 20 cm in diameter × 7–8 cm high. The units were similar in construction to commercial rodent metabolism cages, with the exception that each unit was adjacent to two other units that were built with 1 cm wide "sniff holes" to enable mice to see, sniff, and interact with each other. This is particularly important as mice are highly social and lose condition rapidly when housed in isolation. Mice were housed at all times only with mice of the same gender and strain to avoid potential infection in nude mice and hormonal changes that may impact PK by housing male and female animals in close proximity. Mice were allowed to recover overnight prior to dosing and were weighed once daily.

The following day, mice were weighed and a sample of blank blood (10 µL) collected from the carotid artery cannula via a 0.3-mL syringe fitted with a 31-G needle into heparinized (1 IU) PCR tubes. Mice were then lightly anaesthetized under isoflurane and injected s.c. between the left third and fourth

mammary fat pads with a nominal dose of 4.5 µg PEG–Intron®
in 50 µL saline as a bolus as reported previously or i.v. via a
lateral tail vein over 30 s. This dose was chosen as it is similar
to doses given to mice to explore the antiviral and chemothera-
peutic activity of PEG–Intron®,[15] and therefore reflects the PK
of the cytokine in these PD studies. In addition, PEG–Intron®
did not appear to display nonlinear PK in rats in the previous
study. Blood samples (10 µL) were then collected starting at 5
min after the s.c. dose or 1 min after the end of the i.v. dose,
and further samples were collected at times 0.5, 1, 2, 4, 6, 8, 12,
24, 30, and 48 h. Blood samples were centrifuged at 4000*g* for
5 min to isolate plasma and 5 µL plasma samples were then
mixed with 5 µL saline in 200 µL PCR tubes and stored at
−20°C until analyzed. Standard samples were also prepared in
fresh plasma on the same day and were stored along with the
plasma samples from mice.

The concentrations of PEG–Intron® in mouse plasma were
quantified via ELISA as previously described,[15] and using
dilutions ranging from 1:100 to 1:10,000 in dilution buffer.
The validated concentration range in mouse plasma was
10–1250 pg/mL. The colorimetric assay employed 3,3′,5,5′-
tetramethylbenzidine as the detection reagent, and optical den-
sity was measured at 450 nm on a FluoStar plate reader.

NonCompartmental Analysis

Noncompartmental analysis (NCA) was performed in WinNon-
lin Professional (version 5.2.1; Pharsight Corporation; Prince-
ton, NJ). The area under the plasma concentration–time curve
(AUC) for each profile was calculated using the linear up/log
down method (i.e., the linear trapezoidal rule when concen-
trations are increasing and logarithmic trapezoidal rule when
concentrations are decreasing). The average bioavailability fol-
lowing s.c. dosing (F_{SC}) for each group of mice was calculated
as the ratio of the average dose normalized AUCs extrapolated
to infinity (AUC_{inf}), that is, $F_{SC} = AUC_{inf,SC}/AUC_{inf,i.v.}$; the re-
spective standard deviations were determined via propagation
of errors. The mean absorption time [MAT; representing the
mean residence time (MRT) at the site of injection] following
s.c. dosing was calculated from the MRTs: $MAT = (MRT_{SC}−
MRT_{i.v.})$. All noncompartmental parameters were compared via
one-way ANOVA with a Student Newman Keuls post test for
pairwise multiple comparisons (SigmaPlot version 12.3). Sig-
nificance was determined as $p < 0.05$.

Population PK Modeling

Population modeling was performed utilizing S-ADAPT (ver-
sion 1.57) with the Monte Carlo parametric expectation
maximization algorithm (MC-PEM; importance sampling,
pmethod = 4) and SADAPT-TRAN for preprocessing and
postprocessing.[16,17] Models with two and three disposition com-
partments and first-order s.c. absorption with and without an
additional absorption lag compartment were evaluated. In the
first step of structural model development, the PK profiles fol-
lowing i.v. administration from each group of mice were mod-
eled separately to characterize the distribution and elimination
of PEG–Intron®. In the next step, the i.v. and s.c. PK pro-
files were modeled simultaneously within each group of mice
to determine whether the same model structure applies to all
groups. As the final step of structural model development, all
i.v. and s.c. data from all groups of mice (24 mice in total) were
modeled simultaneously. The interindividual variability (IIV) of

the PK parameters was assumed to be log-normally distributed,
except for F_{SC} that was logistically distributed between 0% and
100%. The residual unidentified variability was described by a
combined additive and proportional error model. The potential
effect of immune status (strain C57Bl/6J vs. nude), gender and
body weight on the PK parameters was systematically evalu-
ated via covariate analysis. Immune status was evaluated as
a categorical covariate, that is, allowing two different typical
values of a parameter for C57Bl/6J and nude mice. Gender was
evaluated accordingly as a categorical covariate. A potential ef-
fect of body weight on clearance and volume parameters was
evaluated for both allometric scaling and linear scaling. A dif-
ference of ≥1.92 in the S-ADAPT objective function ($=-1 ×$ log
likelihood) for one additional degree of freedom was considered
statistically significant according to the chi-square distribu-
tion. Covariate effects were first evaluated for each parameter
separately and then in combination.

Plots of observed versus individual-fitted and observed ver-
sus population-fitted concentrations, visual-predictive checks,
the normalized prediction distribution error, and the objective
function in S-ADAPT were utilized to evaluate model perfor-
mance. For the visual-predictive checks, 12,000 profiles were
simulated for each competing model. The 10th, 25th, 50th, 75th,
and 90th percentiles were calculated from the simulated pro-
files and overlaid on the observed data to compare the central
tendency and the variability of the predicted versus the ob-
served concentrations.

RESULTS

The concentration–time profiles (average ± SD) for each group
of mice following both i.v. and s.c. dosing are presented in
Figure 1. The PEG–Intron® plasma concentrations declined
in a multiexponential fashion after i.v. dosing. Following s.c.
dosing, the concentrations increased to a maximum at 4.0 h for
all female nude mice, 5.5 (±1.0) h for female C57Bl/6J, and 8.0
(±2.8) h for male C57Bl/6J mice and then declined. The max-
imum concentrations (C_{max}) normalized to a 4.5-µg dose were
0.541 (±0.087) µg/mL in female nude, 0.610 (±0.31) µg/mL in
female C57Bl/6J, and 0.284 (±0.051) µg/mL in male C57Bl/6J
mice. The dose- and body weight-normalized C_{max} were 27.0
(±5.16) pg/mL/kg in female nude, 29.8 (±15.6) pg/mL per kg
in female C57Bl/6J, and 9.79 (±2.07) pg/mL per kg in male
C57Bl/6J mice.

The NCA revealed a significantly higher clearance (*$p <$
0.05) in the nude mice group compared with the C57Bl/6J
mice following i.v. dosing (Table 1). There was a trend for
shorter elimination half-life with the nude mice compared with
C57Bl/6J mice; however, this difference was not statistically
significant ($p = 0.12$). No statistically significant differences
in plasma clearance were observed between male and female
C57Bl/6J groups ($p = 0.098$). The volume of distribution at
steady state adjusted for body weight (V_{ss}, L/kg) after i.v. ad-
ministration was significantly greater for the female mice com-
pared with male mice. V_{ss} (L/kg) was highest in nude female
> C57Bl/6J female > C57Bl/6J male (Table 1). No significant
difference in V_{ss} was seen between nude and C57Bl/6J female
groups ($p = 0.21$).

After s.c. administration, a significantly higher MRT (*$p <$
0.02) was observed in C57Bl/6J male mice (16.6 h) than the
female groups (12.8 h vs. 11.0 h for C57Bl/6J and nude mice).
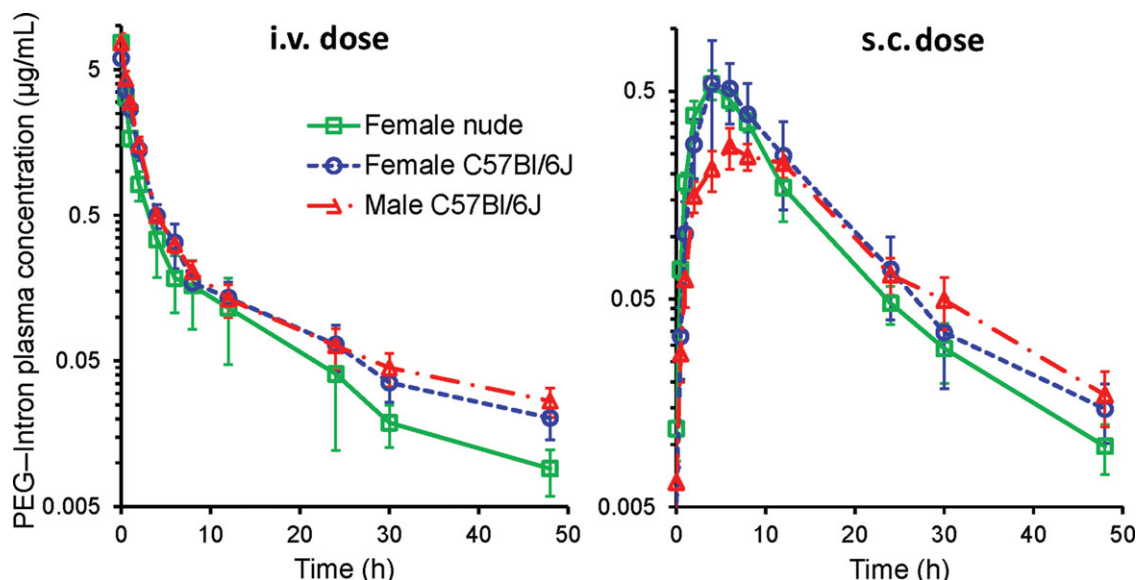
Figure 1. Plasma concentration–time profiles of PEG–Intron® following i.v. and s.c. administration to athymic nude and C57Bl/6J mice. Concentrations are normalized to a dose of 4.5 µg and are presented as average ± standard deviation (SD).

Table 1. Pharmacokinetic Parameters [Average (SD)] from Noncompartmental Analysis

Parameter (Unit)	Route of Administration	Female Nude	Female C57 Bl/6J	Male C57 Bl/6J
CL (mL/h)	i.v.	0.504 (0.11)	0.360 (0.052)	0.329 (0.049)
CL (mL/min per kg)	i.v.	0.432 (0.084)[a]	0.269 (0.039)	0.196 (0.030)
V_{ss} (mL)	i.v.	2.90 (0.34)	2.89 (0.62)	2.74 (0.14)
V_{ss} (L/kg)	i.v.	0.149 (0.013)	0.130 (0.030)	0.0980 (0.0085)[a]
MRT (h)	i.v.	5.92 (1.17)	8.10 (1.72)	8.42 (0.74)
$T_{1/2}$ (h)	i.v.	12.6 (2.9)	16.1 (3.5)	16.7 (1.2)
F_{SC} (%)	s.c.	65.7 (18)[b]	55.6 (21)	38.8 (6.9)[b]
MRT (h)	s.c.	11.0 (1.1)	12.8 (2.1)	16.6 (2.3)[a]
MAT (h)	s.c.	5.1 (1.6)	4.7 (2.7)	8.2 (2.4)
$T_{1/2}$ (h)	s.c.	9.9 (2.8)	10.3 (3.1)	11.5 (2.6)

[a]Statistically significant difference ($p < 0.05$) between this group and other groups.
[b]Statistically significant difference ($p < 0.05$) between these two groups.
CL, total body clearance; V_{ss}, volume of distribution at steady state; MRT, mean residence time; $T_{1/2}$, terminal half-life; F_{SC}, bioavailability of s.c. versus i.v. dosing; MAT, mean absorption time.

No significant difference in MRT was observed between the two female groups ($p = 0.23$). The absolute bioavailability after s.c. administration (F_{SC}) was higher in females than in males and highest in the female nude mice. There was significant difference in F_{SC} in nude female mice compared with C57Bl/6J male mice (**$p < 0.01$). There was a trend in F_{sc} between the two groups of female mice indicating that bioavailability was greater in the nude strain than in the C57Bl/6J strain; however, this was not statistically significant ($p = 0.052$). No significant difference in F_{sc} was observed between male and female C57Bl/6J mice ($p = 0.19$). The MAT following s.c. dosing was approximately 1.7-fold longer in male than in female mice (Table 1). No significant difference in half-life was observed after s.c. administration in all groups ($p = 0.707$).

A population model with three disposition compartments (linear elimination and first-order absorption with a lag compartment) successfully described all i.v. and s.c. profiles within each group (Fig. 2). When all data were modeled simultaneously without considering potential effects of immune status and gender on the PK parameters, the model predictions were systematically biased. For example, the concentrations in the terminal
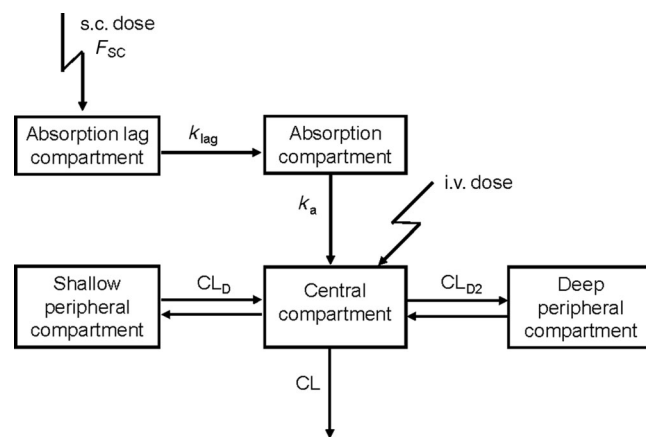
Figure 2. Model diagram. Parameter abbreviations are explained in the legend of Table 2.

phase following i.v. and s.c. dosing in female nude mice were overpredicted, the C_{max} following s.c. dosing in female nude and
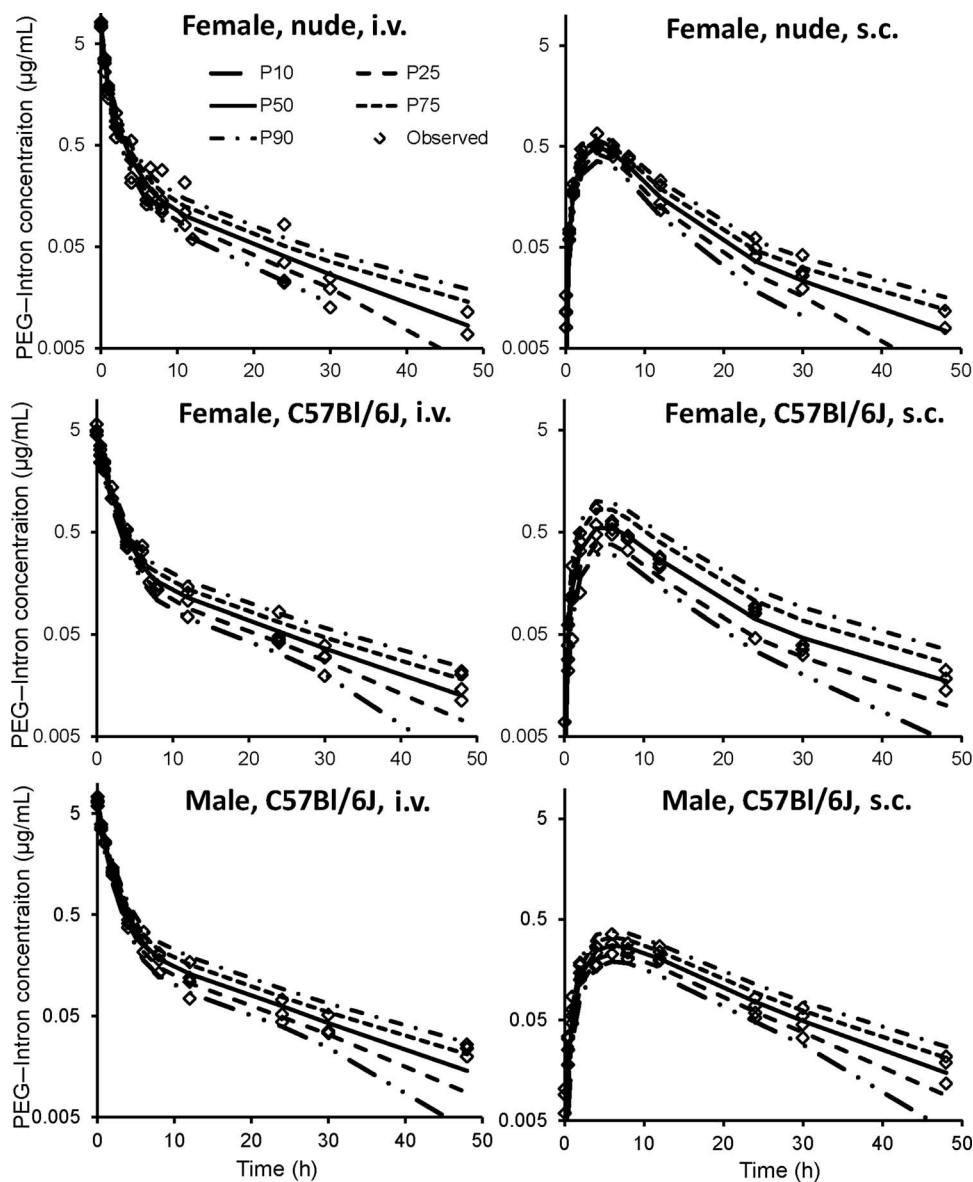
Figure 3. Visual-predictive checks of the final model including covariate effects, stratified by gender, strain, and route of administration. The diamonds represent the observed concentrations. The lines represent the model-predicted 10th percentile (lower broken and dotted line), 25th percentile (lower broken line), median (solid line), 75th percentile (upper broken line), and 90th percentile (upper broken and dotted line).

C57Bl/6J mice were considerably underpredicted, and the $C_{\max}$ following s.c. dosing in male C57Bl/6J mice substantially over-predicted. The final model that included the statistically significant covariate relationships achieved very good-predictive performance as evidenced by visual-predictive checks (Fig. 3).

The PK parameter estimates from the final model including covariate effects are presented in Table 2. Inclusion of allometric or linear effects of body weight on clearance and volume parameters was evaluated, but did not result in an improved objective function or a decrease in the unexplained IIV. Therefore, the population PK parameter estimates in the text and in Table 2 are not adjusted for body weight. Each of the covariate relationships in the final model (except for the effect on F_{SC}) was statistically significant ($p < 0.05$), both separately and in addition to the other included covariate effects, and led to a

decrease in the unexplained IIV of the parameter estimates compared with the model without covariates. The higher F_{SC} in females compared with males was not statistically significant. However, including this effect substantially improved the predictive performance of the model for the female nude and male C57Bl/6J mice following s.c. dosing. Our detailed covariate analysis indicated a 27% higher ($p < 0.05$) total body clearance in nude compared with C57Bl/6J mice (Table 2). The central volume of distribution (V_1) was higher in the C57Bl/6J than in nude mice, whereas the shallow peripheral volume of distribution (V_2) was twofold higher in the nude mice. The absorption rate constant (k_a) was higher in nude than C57Bl/6J mice and considerably higher in females than males. Inclusion of covariate effects on other parameters was not statistically significant.

Table 2. Population Mean Estimates, Standard Errors (SE) and Inter-Individual Variability (IIV) of the Final Model with Covariate Effects

Parameter (Unit)	Population Mean (SE [%CV])	IIV (%CV or 5th–95th Percentile)	Female Nude (SE%)	Female C57Bl/6J (SE%)	Male C57Bl/6J (SE%)
CL (mL/h)	0.430	13.3	0.503 (6.27)	0.397 (4.72)	
V_1 (mL)	0.652	2.52	0.564 (4.26)	0.755 (3.84)	0.652 (4.41)
V_2 (mL)	0.215	11.6	0.352 (19.1)	0.168 (15.1)	
V_3 (mL)	2.05 (6.53)	10.2	.	.	.
CL_D (mL/h)	0.378 (27.5)	22.0	.	.	.
CL_{D2} (mL/h)	0.198 (7.18)	19.4	.	.	.
k_{lag} (h^{-1})	0.457 (13.6)	23.2	.	.	.
k_a (h^{-1})	0.242	12.2	0.374 (16.4)	0.274 (13.5)	0.138 (11.9)
F_{SC} (%)	56.0	40.0–70.8	60.8 (47.9)		46.2 (172)
SDCP (µg/mL)	0.00562 (13.4)	.	.	.	.
CVCP (%)	10.8 (8.45)	.	.	.	.

CL, total body clearance; V_1, central volume of distribution; V_2, shallow peripheral volume of distribution; V_3, deep peripheral volume of distribution; CL_D, intercompartmental clearance between central and shallow peripheral compartment; CL_{D2}, intercompartmental clearance between central and deep peripheral compartment; k_{lag}, first-order rate constant describing the lag time of absorption; k_a, first-order rate constant of absorption into the central compartment; F_{SC}, bioavailability following s.c. administration; SDCP, additive residual error; CVCP, proportional residual error.

DISCUSSION

The time course of drug concentrations and effects can be systematically influenced by many subject or animal characteristics, such as gender, immune status, renal function, body weight, and age. Although these principles are well-established in the human clinical setting,[18–20] their application within the preclinical setting, particularly with respect to studies conducted in rodents, often appears to be neglected. However, rodent models are an invaluable and extensively utilized tool in drug development and translational pharmacology and are a fundamental precursor to studies conducted in man. For practical reasons, different strains of animals from within one species and even different species may be used in various stages of preclinical drug development, for example, PK, PD, and disease progression studies. Quantifying the influence of using animals with different characteristics such as gender and immune status on the observed drug concentrations and effects is therefore important for interpretation and translation of the results between these studies.

The observed PK profiles from our study were evaluated by two different data analytical approaches. The NCA provided individual PK parameters that were subjected to descriptive statistics and compared between the different groups of mice (Table 1). In contrast, population modeling and covariate analysis directly estimate the true biological variability between animals or patients and can distinguish between random heterogeneity and systematic variability because of specific characteristics. We developed a population PK model (Fig. 2) to quantitatively describe and predict plasma concentration–time profiles of PEG–Intron® following i.v. and s.c. administration in female and male, and immunocompromised and immunocompetent mice. PEG–Intron® displayed linear PK for all groups and routes of administration at the studied dose. The s.c. absorption was best described by two sequential first-order processes, that is, including a lag or depot compartment from which PEG–Intron® transfers into the absorption compartment and subsequently into the systemic circulation (central compartment). The lag compartment for s.c. absorption was required in all three groups of mice.

Both interferon-α (IFN-α) and IFN-β bind to the receptors IFNAR1 and IFNAR2.[21] These receptors are distributed throughout most cells and tissues of the body (in particular immune cells) with the exception of low, or nondetectable levels in erythrocytes, the kidney, brain, central nervous system, and platelets. A soluble form of IFNAR2 is present in serum and may contribute to the PK of IFN-α and IFN-β.[22] With regards to the impact of IFN receptor binding in dictating the PK and distribution of interferons, non-PEGylated IFN-β1a was previously described as exhibiting target-mediated drug disposition because of saturable high-affinity binding to its receptor in humans and monkeys.[23,24] In contrast, PEGylated IFN-β1a was successfully described by a model with linear elimination,[25] potentially because of the decreased receptor binding affinity conferred by the PEG chain. Similarly, PEGylated IFN-α2b (PEG–Intron®) and albinterferon-α2b have been successfully described by models with linear elimination.[12,13,26,27] In the present study, the plasma PK of PEGylated human interferon-α2 was examined in mice, which have a low IFN sequence identity to humans. In addition, our previous study indicated that human IFN-α2b was unable to promote cancer immunosurveillance by mouse white blood cells,[28] suggesting that in the current study, the plasma PK of PEG–Intron® was unlikely to have been significantly influenced by receptor interactions.

Although the PK in all groups of mice followed the same general structural model, systematic differences in the PK parameter estimates were identified between the groups with both data analytical approaches. For instance, a significantly higher clearance in immunocompromised female nude versus female and male immunocompetent C57Bl/6J mice was identified both by NCA and population modeling (Tables 1 and 2). Although we did not explore the mechanisms behind these PK differences, data in humans suggest that renal elimination accounts for approximately 30% of PEG–Intron® clearance, whereas the remaining fraction is eliminated by hepatic metabolism and intracellular degradation.[29,30] Differences in renal metabolism and elimination are unlikely; however, previous reports have suggested that nude rats and mice display differences in macrophage function and activity when compared with immunocompetent rodents. Thus, the uptake of macromolecules by the liver and spleen (major organs of the MPS) is significantly higher in nude when compared with fully immunocompetent animals. Therefore, it is likely that a potential contributing factor to the higher clearance in nude mice might

be the difference in the number and type of T-lymphocytes between nude and C57Bl/6J mice, which appears to impact on macrophage activity.[9] In addition, as PEG–Intron® acts primarily on NK cells, T-cells, and macrophages (interferons),[31,32] it is likely that differences in the population of these cells between nude and immunocompetent mice had an impact on cellular uptake and intracellular metabolism.

A trend was also observed toward a higher plasma clearance of PEG–Intron® in female compared with male C57Bl/6J mice (Table 1). Although the basis of this is not known, it is interesting to note that the trend is consistent with the observed trend in PEG–Intron® clearance in chronic hepatitis C patients, where gender was a significant covariate and apparent clearance following s.c. administration was higher in females than males.[13] Similarly, Gupta et al.[12] found that including the effect of gender in a population PK model of PEG–Intron® in male and female patients with chronic myelogenous leukemia (with suppressed immune function) was significant compared with the model without covariate effects ($p < 0.02$). Although the most significant covariate was creatinine clearance ($p < 0.0001$), which was calculated based on gender, body weight, age, and serum creatinine concentration, gender had the largest effect out of the four variables used for calculating creatinine clearance.[12] Furthermore, sustained virological response of PEG–Intron® is also higher in postmenopausal women, and this has been attributed to altered PK behavior as a result of lower estrogen that enhances the exposure of visceral fat to the cytokine.[14]

The considerably slower rate of absorption in male compared with female animals that we found by population modeling is reflected in the approximately 1.7-fold higher MAT in males calculated by NCA. Both approaches also identified a higher extent of absorption in females than in males. Again, the mechanism(s) underlying this difference in absorption rate between genders is not known; however, it is tempting to speculate that it may be because of differences in the fat content at the s.c. injection site, particularly given that the size and shape of fat lobules in the s.c. tissue was also found to be dependent on gender in humans.[33] Additionally, PEG–Intron® was reported in a previous study to be absorbed from an s.c. injection site largely via the lymph, suggesting that differences in lymphatic physiology and exposure between male and female animals would likely impact on absorption from the s.c. space.[15] To this end, we recently reported that male and female C57Bl/6J mice display differences in thoracic lymph duct physiology.[3] Similarly, others have observed differences in lymphatic physiology and function in humans.[34,35] Similar differences in the overall body composition between genders and strains may also have contributed to the observed differences in the central (V_1) and shallow peripheral (V_2) volumes of distribution (Table 2), even though the model-derived volume of distribution at steady state [V_{ss}; being the sum of V_1 and the two peripheral (V_2, V_3) volumes of distribution] and V_{SS} based on the NCA were similar between the groups, unless normalized by body weight (Table 1).

Overall, we have identified significant differences in the PK parameters for PEG–Intron® between female and male and immunocompromised and immunocompetent mice. These differences in PK parameter estimates were identified by two different approaches, providing a high degree of confidence to the results, and significance between the groups was identified using a relatively small number of animals per group. The developed population PK model including covariate relationships

may be used to predict the concentration–time profiles for other doses and dosage regimens than those administered in the current study in the three different groups of mice. Thereby, the model can contribute to optimizing the design of future *in vivo* efficacy/safety studies. By combining this model with a PD model, the effects of different PK characteristics on the drug effects can be described and predicted. Finally, although a direct translation of the current work to predict the disposition of PEG–Intron® in humans is beyond the scope of the present work, this work serves to demonstrate that quantitative assessment of the effects of gender and immune status (and potentially other factors) can be readily applied within a preclinical setting, including the development of macromolecular drugs.

REFERENCES

1. Regitz-Zagrosek V, Seeland U. 2012. Sex and gender differences in clinical medicine. Handb Exp Pharmacol 214:3–22.
2. Schiebinger L. 2014. Scientific research must take gender into account. Nature 507:9.
3. Caliph SM, Shackleford D, Ascher DB, Kaminskas LM. 2015. Practical lessons in murine thoracic lymph duct cannulations: Observations in female and male mice across four different strains that impact on 'cannulatability'. J Pharm Sci 104(3):1207–1209.
4. Makhmudov ZA. 1980. [Sex characteristics of the anatomy of the superior mesenteric lymph nodes in an adult]. Arkh Anat Gistol Embriol 79:63–66.
5. Richter WF, Bhansali SG, Morris ME. 2012. Mechanistic determinants of biotherapeutics absorption following SC administration. AAPS J 14:559–570.
6. La-Beck NM, Wu H, Infante JR, Jones SF, Burris HA, Keedy VL, Kodaira H, Ikeda S, Ramanathan RK, Zamboni W. 2010. The evaluation of gender on the pharmacokinetics (PK) of pegylated liposomal anticancer agents. J Clin Oncol 28:e13003.
7. Sapino A, Cassoni P, Ferrero E, Bongiovanni M, Righi L, Fortunati N, Crafa P, Chiarle R, Bussolati G. 2003. Estrogen receptor alpha is a novel marker expressed by follicular dendritic cells in lymph nodes and tumor-associated lymphoid infiltrates. Am J Pathol 163:1313–1320.
8. Maeda H. 2012. Macromolecular therapeutics in cancer treatment: the EPR effect and beyond. J Control Release 164:138–144.
9. Vaessen LMB, Broekhuizen R, Rozing J, Vos JG, Schuurman HJ. 1986. T-cell development during aging in congenitally athymic (nude) rats. Scand J Immunol 24:223–235.
10. Kaminskas LM, Kelly BD, McLeod VM, Boyd BJ, Krippner GY, Williams ED, Porter CJ. 2009. Pharmacokinetics and tumor disposition of PEGylated, methotrexate conjugated poly-l-lysine dendrimers. Mol Pharm 6:1190–1204.
11. Mamede M, Saga T, Ishimori T, Nakamoto Y, Sato N, Higashi T, Mukai T, Kobayashi H, Konishi J. 2003. Differential uptake of (18)F-fluorodeoxyglucose by experimental tumors xenografted into immunocompetent and immunodeficient mice and the effect of immunomodification. Neoplasia 5:179–183.
12. Gupta S, Jen J, Kolz K, Cutler D. 2007. Dose selection and population pharmacokinetics of PEG–Intron in patients with chronic myelogenous leukaemia. Br J Clin Pharmacol 63:292–299.

13. Xu C, Gupta S, Krishna G, Cutler D, Wirth S, Galoppo C, Ciocca M, Kolz K, Noviello S, Sniukiene V. 2013. Population pharmacokinetics of peginterferon alfa-2b in pediatric patients with chronic hepatitis C. Eur J Clin Pharmacol 69:2045–2054.

14. Villa E, Camma C, Di Leo A, Karampatou A, Enea M, Gitto S, Bernabucci V, Losi L, De Maria N, Lei B, Ferrari A, Vukotic R, Vignoli P, Rendina M, Francavilla A. 2012. Peginterferon-alpha_2B plus ribavirin is more effective than peginterferon-alpha_2A plus ribavirin in menopausal women with chronic hepatitis C. J Viral Hepat 19:640–649.

15. Kaminskas LM, Ascher DB, McLeod VM, Herold MJ, Le CP, Sloan EK, Porter CJH. 2013. PEGylation of interferon alpha2 improves lymphatic exposure after subcutaneous and intravenous administration and improves antitumour efficacy against lymphatic breast cancer metastases. J Control Release 168:200–208.

16. Bulitta JB, Bingolbali A, Shin BS, Landersdorfer CB. 2011. Development of a new pre- and post-processing tool (SADAPT-TRAN) for nonlinear mixed-effects modeling in S-ADAPT. AAPS J 13:201–211.

17. Bulitta JB, Landersdorfer CB. 2011. Performance and robustness of the Monte Carlo importance sampling algorithm using parallelized S-ADAPT for basic and complex mechanistic models. AAPS J 13:212–226.

18. Bulitta JB, Landersdorfer CB, Forrest A, Brown SV, Neely MN, Tsuji BT, Louie A. 2011. Relevance of pharmacokinetic and pharmacodynamic modeling to clinical care of critically ill patients. Curr Pharm Biotechnol 12:2044–2061.

19. Neely MN, Rakhmanina NY. 2011. Pharmacokinetic optimization of antiretroviral therapy in children and adolescents. Clin Pharm 50:143–189.

20. Roberts JA, Abdul-Aziz MH, Lipman J, Mouton JW, Vinks AA, Felton TW, Hope WW, Farkas A, Neely MN, Schentag JJ, Drusano G, Frey OR, Theuretzbacher U, Kuti JL, International Society of Anti-Infective P, the P, Pharmacodynamics Study Group of the European Society of Clinical M, Infectious D. 2014. Individualised antibiotic dosing for patients who are critically ill: Challenges and potential solutions. Lancet Infect Dis 14:498–509.

21. Mogensen KE, Lewerenz M, Reboul J, Lutfalla G, Uze G. 1999. The type I interferon receptor: Structure, function, and evolution of a family business. J Interferon Cytokine Res 19:1069–1098.

22. de Weerd NA, Nguyen T. 2012. The interferons and their receptors—Distribution and regulation. Immunol Cell Biol 90:483–491.

23. Mager DE, Jusko WJ. 2002. Receptor-mediated pharmacokinetic/pharmacodynamic model of interferon-beta 1a in humans. Pharm Res 19:1537–1543.

24. Mager DE, Neuteboom B, Efthymiopoulos C, Munafo A, Jusko WJ. 2003. Receptor-mediated pharmacokinetics and pharmacodynamics of interferon-beta1a in monkeys. J Pharmacol Exp Ther 306:262–270.

25. Mager DE, Neuteboom B, Jusko WJ. 2005. Pharmacokinetics and pharmacodynamics of PEGylated IFN-beta 1a following subcutaneous administration in monkeys. Pharm Res 22:58–61.

26. Riggs MM, Bergsma TT, Rogers JA, Gastonguay MR, Subramanian GM, Chen C, Devalaraja M, Corey AE, Sun H, Yu J, Stein DS. 2012. Population pharmacokinetics and exposure-response of albinterferon alfa-2b. J Clin Pharmacol 52:475–486.

27. Rozenberg L, Haagmans BL, Neumann AU, Chen G, McLaughlin M, Levy-Drummer RS, Masur H, Dewar RL, Ferenci P, Silva M, Viola MS, Polis MA, Kottilil S. 2009. Therapeutic response to peg-IFN-alpha-2b and ribavirin in HIV/HCV co-infected African-American and Caucasian patients as a function of HCV viral kinetics and interferon pharmacodynamics. AIDS 23:2439–2450.

28. Kaminskas LM, Ascher DB, McLeod VM, Herold MJ, Le CP, Sloan EK, Porter CJ. 2013. PEGylation of interferon alpha2 improves lymphatic exposure after subcutaneous and intravenous administration and improves antitumour efficacy against lymphatic breast cancer metastases. J Control Release 168:200–208.

29. Ahn J, Flamm S. 2004. Peginterferon-alpha(2b) and ribavirin. Expert Rev Anti Infect Ther 2:17–25.

30. PEG–Intron prescribing information. Accessed on December 22, 2014, at: http://www.pegintron.com/peg/pegintron/consumer/index.jsp.

31. Malaponte G, Passero E, Leonardi S, Monte V, Lauria C, Mazzarino C, Sciotto A, Russo Mancuso G, Di Gregorio F, Musumeci S. 1997. Effect of alpha-interferon on natural killer cell activity and lymphocyte subsets in thalassemia patients with chronic hepatitis C. Acta Haematol 98:83–88.

32. Ikeda H, Old LJ, Schreiber RD. 2002. The roles of IFN gamma in protection against tumor development and cancer immunoediting. Cytokine Growth Factor Rev 13:95–109.

33. Mirrashed F, Sharp JC, Krause V, Morgan J, Tomanek B. 2004. Pilot study of dermal and subcutaneous fat structures by MRI in individuals who differ in gender, BMI, and cellulite grading. Skin Res Technol 10:161–168.

34. Unno N, Tanaka H, Suzuki M, Yamamoto N, Mano Y, Sano M, Saito T, Konno H. 2011. Influence of age and gender on human lymphatic pumping pressure in the leg. Lymphol 44:113–120.

35. Shvetsov EV. 1991. [Anatomy and topography of external iliac lymph nodes in adults]. Arkh Anat Gistol Embriol 100:50–57.